

Constituent Quarks and Multi-strange Baryon Production in Heavy-Ion Collisions

Nirbhay K. Behera¹, Raghunath Sahoo^{2*}, Basanta K. Nandi¹

¹*Indian Institute of Technology Bombay, Mumbai, India-40007 and*

²*Indian Institute of Technology Indore, Indore, India-452017*

(Dated: June 29, 2012)

In the frame work of the nuclear overlap model, we estimate the number of nucleon and quark participants in proton-proton, proton-nucleus and nucleus-nucleus collisions. We observe the nucleon normalized yield of multi-strange particles which show a linear rise with centrality, turns out to be a centrality independent scaling behavior when normalized to number of constituent quarks participating in the collision. This geometrical scaling indicates the partonic degrees of freedom playing important role in the production of multi-strange particles. Furthermore, we observe the constituent quark normalized yield when normalized to the strangeness content, it shows a strangeness independent scaling behavior. We give a comparison of data with HIJING, AMPT and UrQMD models to understand the particle production dynamics.

PACS numbers: 25.75.Ld

Keywords: constituent quarks, multi-strange baryons, QGP, strangeness scaling

I. INTRODUCTION

Relativistic heavy-ion collisions aim at creating matter at extreme conditions of energy density and temperature which is governed by the partonic degrees of freedom called Quark-Gluon Plasma (QGP). The main focus of these studies are the observation of quark-hadron phase transition and exploring the Quantum Chromodynamics (QCD) phase diagram. In the early phases of ultra-relativistic heavy-ion collisions, when a hot and dense region is formed in the core of the reaction zone, different quark flavors are produced. Then the produced matter undergoes transverse expansion and multiple scattering among the produced particles. The formation of the hadrons from the partonic phase is accomplished through further expansion and cooling of the system. In proton-proton ($p+p$) collisions, the formation of QGP is not expected, whereas a possible formation of QGP is expected in nucleus-nucleus (A+A) collisions. Hence, a comparative study of produced particles in A+A collisions, with that of $p+p$ collisions, could give better understanding of the properties of the medium formed in A+A collisions.

In the mid-rapidity region, strangeness enhancement has been proposed as a potential signature of QGP [1, 2]. Strange baryons are produced in strong interaction processes and decay through weak interaction. It has been observed that multi-strange baryons, $\Omega(sss)$, $\Xi(ssd)$ and $\Lambda(uds)$, are formed and decouple from the system earlier in time [3]. Due to their different reaction rates in the medium, particles with different strangeness decouple at different times. Relativistic Quantum Molecular Dynamics (RQMD) results suggest that the multi-strange baryons freeze-out at energy densities more than

$1 \text{ GeV}/fm^3$ [3] which corresponds to the critical energy density predicted by lattice QCD calculations [4]. The study of multi-strange baryons are of paramount importance in high energy heavy-ion collisions because of their dominant strangeness content (s-quark). As the colliding species in nuclear collisions do not contain any strange valence quark, particles with non-zero strange quarks can only be produced out of the collision process. The production of strange particles is enhanced in a QGP phase compared to a hadronic system. This is because, the production rate of $gg \rightarrow s\bar{s}$ is high in a QGP medium [5], which is absent in hadronic phase. In addition, multi-strange baryons are less suffered by hadronic rescatterings in the later stage of the evolution of the fireball because of their small hadronic interaction cross sections. That is why multi-strange hadrons are good probes to carry the early stage information [6–10]. Hydrodynamic model estimations on hadron p_T spectra suggest that the thermal freeze-out temperature of multi-strange baryons are close to their chemical freeze-out temperature ($T_{ch} \sim 160 \text{ MeV}$), which is around the critical temperature, T_c , for deconfinement transition. This indicates that multi-strange baryons are almost not affected by hadronic rescatterings at the later stage of the heavy-ion collisions [6, 9]. Hence, multi-strange baryons could carry the information of possible formation of a QGP phase. It could be envisaged that the multi-strange baryons are formed out of partonic interactions rather than nucleonic interactions. We shall be justifying this in the following sections.

In this paper, both nuclei and nucleons are considered as superposition of constituent or “dressed” quarks (partons or valons). There are three constituent quarks per nucleon. Baryons are composed of three and mesons are of two such quarks. The concept of constituent quarks is very well known [11, 12] and established in the realm of the discovery of constituent quark scaling of identi-

*Corresponding Author, Email: Raghunath.Sahoo@cern.ch

fied particles elliptic flow at RHIC [13]. The constituent quark approach is successful in explaining many features of hadron-hadron, hadron-nucleus [14] and nucleus-nucleus collisions. These include global properties like the charged particle and transverse energy density per participant pair [15, 16]. QCD calculations support the presence of three objects of size 0.1-0.3 fm inside a nucleon [17]. Furthermore, it has been seen that nucleus-nucleus collisions and $p + p$ collisions have similar initial states if the results are scaled by the number of constituent quark participants [18]. These observations also indicate that the particle production is essentially controlled by number of constituent quarks pairs participating in the collision. In a constituent quark picture, nucleon-nucleon (NN) collision looks like a collision of two light nuclei with essentially one qq pair interacting in the collision, leaving other quarks as spectators. These quark spectators form hadrons in the nucleon fragmentation region with a part of the entire nucleon energy being used for the particle production ($\sqrt{s_{qq}} \sim \sqrt{s_{NN}}/3$). But in A+A collisions, due to the large size of the nucleus compared to the nucleon, there is a higher probability of $q - q$ interaction between the projectile and target nucleons. It has been observed at RHIC energies that the production rate of strange and multi-strange baryons in Au+Au collisions at $\sqrt{s_{NN}} = 200$ GeV, when scaled by the number of nucleon participants, are different (get enhanced) when compared to similar measurements in $p + p$ collisions at same energy [20]. The observed enhancement increases with strangeness content of the baryons and also as a function of collision centrality, while going from peripheral to central collisions. Similar observations have been made at SPS energy for Pb+Pb collisions at $\sqrt{s_{NN}} = 17.3$ GeV, when compared with the corresponding measurements for p+Be collisions at the same energy [21]. In this paper, we have compared the centrality dependence of number of nucleon participant normalized multi-strange baryon enhancement at SPS and RHIC energies with the expectations from HIJING, AMPT and UrQMD models. The linear rise of the enhancement seen in the data, gets converted into a spectacular quark-participant scaling behavior when normalized to number of quark-participants. Furthermore, we explore the strangeness scaling, where quark-participant normalized enhancement for different multi-strange baryons, when divided by the strangeness content show a strangeness-independent scaling behavior.

II. CALCULATION OF THE NUMBER OF PARTICIPANTS

The calculations of the mean number of nucleon/quark participants are done in the following way. In the nuclear overlap model, the mean number of participants, i.e. N_{N-part} , in the collisions of a nucleus A and a nu-

cleus B with impact parameter b is given by

$$N_{N-part,AB} = \int d^2s T_A(\vec{s}) \{1 - [1 - \frac{\sigma_{NN} T_B(\vec{s} - \vec{b})}{B}]^B\} + \int d^2s T_B(\vec{s}) \{1 - [1 - \frac{\sigma_{NN} T_A(\vec{s} - \vec{b})}{A}]^A\}, \quad (1)$$

where $T(b) = \int_{-\infty}^{\infty} dz n_A(\sqrt{b^2 + z^2})$ is the thickness function, defined as the probability of having a nucleon-nucleon (NN) collision within the transverse area element db . $[1 - \sigma_{NN} T_A(b)/A]^A$ is the probability for a nucleon to pass through the nucleus without any collision. A and B are the mass numbers of two nuclei participating in the collision process. We use the Woods-Saxon nuclear density profile,

$$n_A(r) = \frac{n_0}{1 + \exp[(r - R)/d]}, \quad (2)$$

with parameters, the normal nuclear density $n_0 = 0.17 \text{ fm}^{-3}$, the nuclear radius $R = (1.12A^{1/3} - 0.86^{-1/3}) \text{ fm}$ and the skin depth $d = 0.54 \text{ fm}$. The inelastic nucleon-nucleon cross sections, i.e. σ_{NN} , are 42 mb at $\sqrt{s_{NN}} = 200 \text{ GeV}$ and 30 mb at $\sqrt{s_{NN}} = 17.3 \text{ GeV}$. Considering proton as a point particle and nucleus as an extended object in a $p + A$ collision, the number of participating nucleons is given by

$$N_{N-part,pA} = \{1 - [1 - \frac{\sigma_{NN} T_A(b)}{A}]^A\} + T_A(b) \sigma_{NN}. \quad (3)$$

In order to calculate the number of quark participants, N_{q-part} , in nucleus-nucleus collisions, the density for quarks inside the nucleus is changed to three times that of the nucleon density ($n_0^q = 3n_0 = 0.51 \text{ fm}^{-3}$). Instead of nucleon-nucleon cross section, quark-quark cross section is used which is 4.67 mb and 3.3 mb at $\sqrt{s_{NN}} = 200 \text{ GeV}$ and 17.3 GeV, respectively [15, 22]. In $p + p(\bar{p})$ collisions, the quark participants are calculated by considering the proton and antiproton as hard sphere of radius 0.8 fm [23]. And for asymmetric collisions, like $p + A$ collisions, proton is considered as a hard sphere of radius 0.8 fm and nucleus as extended objects with a Woods-Saxon density profile.

III. RESULTS AND DISCUSSION

At lower center of mass energies, it has been found that the particle production scales with the number of participating nucleons, contrary to the case of high energies where hard processes dominate. Hard processes have much smaller cross-section than the soft processes. However, the number of binary collisions increase with increase in collision centrality faster than the number of participants. As a result, the particle production per participant nucleon increases with centrality. By

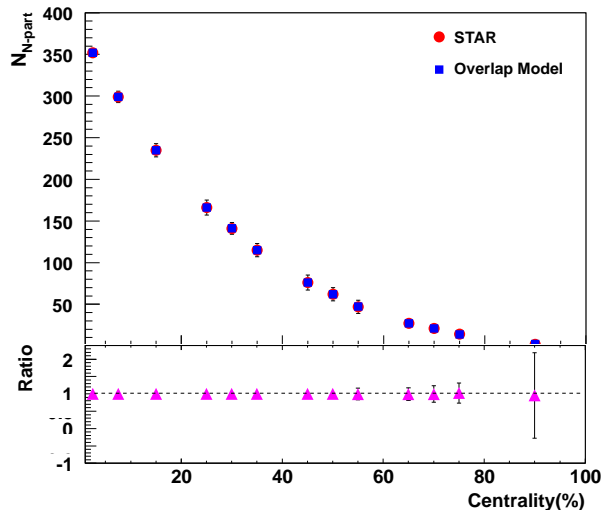


FIG. 1: (Color online) Mean number of nucleon participants as a function of centrality in the overlap model (filled square) and from STAR calculations (filled circles).

using constituent quark approach, we are going to show how the particle production at higher energies depends on the participating quarks. For this, multi-strange particles are chosen because of the proposed signature of strangeness enhancement in QGP medium. This enhancement is due to high production rate of $gg \rightarrow s\bar{s}$ in QGP and it can be explained in the context of statistical mechanics. In $p + p$ system, the strangeness enhancement is not expected as the available volume is much smaller compared to nucleus-nucleus system. The $p + p$ system can be treated as canonical system and the net strangeness number should be conserved. So the $s\bar{s}$ pairs are created at the same point and are annihilated as well, resulting in the suppression of strange hadrons. But in Au+Au system, strange and anti-strange hadrons are created independently and statistically distributed over the entire nuclear fireball, which could be treated in a grand canonical ensemble approach (GC) [19]. As the system thermalizes, the phase space suppression disappears as the volume available is more. The volume here is linearly proportional to the number of participating nucleons, *i.e.* N_{N-part} . So a relative strangeness enhancement is observed in Au+Au collisions with respect to $p + p$ collisions [20]. To study the constituent quarks dependence of strangeness enhancement, we need to estimate the number of participating quarks, which has been done in the framework of nuclear overlap model.

Since the quark participants are calculated in the framework of nuclear overlap model, it is very essential to check how good is our estimation of number of par-

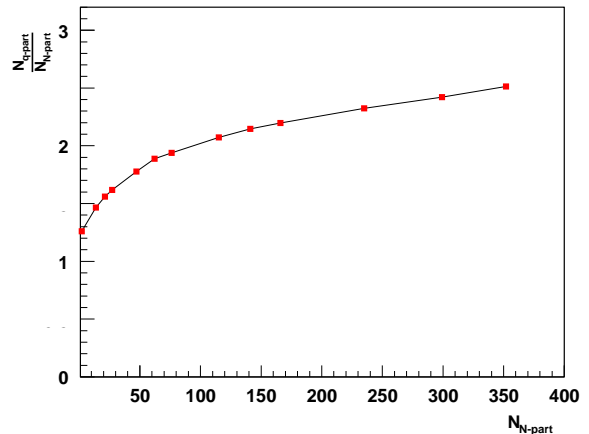


FIG. 2: (Color online) The ratio of N_{q-part}/N_{N-part} as a function of centrality for Au+Au collisions at $\sqrt{s_{NN}} = 200$ GeV from the overlap model calculations.

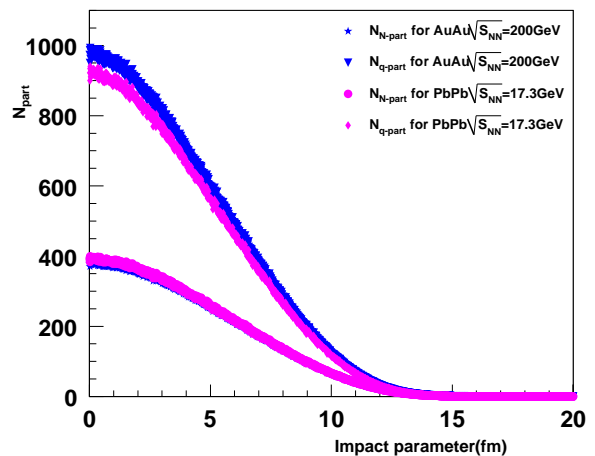


FIG. 3: (Color online) Mean number of nucleon and quark participants as a function of impact parameter from the overlap model calculations for Pb+Pb and Au+Au collisions at SPS and RHIC top energies.

ticipating nucleons in the collision. In order to do that, the mean number of participating nucleons, calculated in overlap model, are compared with the number estimated by the STAR experiment [24]. In Figure 1, the mean number of participating nucleons are shown as a function of collision centrality. Solid circles represent the STAR values and the solid squares represent the overlap model calculations. The lower panel of Figure 1, represents the ratio of STAR values and the overlap model values. It is clear from the figure that the overlap model calculations are in good agreement with the STAR calculations. We have then estimated the number of quark participants within the prescription described in the previous section. The ratio of quark participants and nucleon participants is

shown in Figure 2 as a function of nucleon participants. The ratio shows a sharp increase for $N_{N-part} \leq 100$ and then shows a type of linear rise going from peripheral to central collisions. In Figure 3, we compare the number of nucleon and quark participants for Au+Au collisions at $\sqrt{s_{NN}} = 200$ GeV and for Pb+Pb collisions at $\sqrt{s_{NN}} = 17.3$ GeV as a function of collision impact parameter.

The yield enhancement factor, $E(i)$, for particle species i is given by

$$E(i) = \frac{Yield^{AA}(i) \langle N_{N-part}^{NN} \rangle}{Yield^{NN}(i) \langle N_{N-part}^{AA} \rangle}, \quad (4)$$

where, $Yield^{AA}(i)$ and $Yield^{NN}(i)$ are the yields of strange particles in nucleus-nucleus and nucleon-nucleon collisions, respectively. N_{N-part}^{NN} and N_{N-part}^{AA} are the number of nucleon participants in nucleon-nucleon and nucleus-nucleus collisions, respectively. The number of nucleon participants, i.e. N_{N-part} , is used to characterize the collision centrality. However, in the constituent quark framework, the nucleon participants no longer bear the meaning of sources of particle production. It is assumed that, in this picture the constituent quarks are participating in the reaction and are the sources of interest for particle production. To understand the collision dynamics, the collision data are compared with models like HIJING-1.35, AMPT (default version) and UrQMD-3.3p1. HIJING is a Heavy Ion Jet Interaction Generator which includes multiple minijet production, nuclear shadowing of parton distribution functions and the mechanism of jet interaction with dense matter. This model is based on perturbative QCD [25]. Motivated by perturbative QCD, AMPT (A Multi-Phase Transport) model includes both initial partonic and final state hadronic interactions with quark-gluon to hadronic matter transition and their space-time evolution. Here, the partons are allowed to undergo scattering before they hadronize [26]. UrQMD (Ultra-relativistic Quantum Molecular Dynamics) model is based on microscopic transport theory, where hadronic interactions play an important role describing the evolution of the system [27].

In Figure 4, N_{N-part} -normalized enhancement of Λ and $\bar{\Lambda}$ -baryons for Au+Au collisions at $\sqrt{s_{NN}} = 200$ GeV are shown as a function of N_{N-part} . This collision data are from the STAR experiment [20] and are compared with the corresponding estimates of HIJING, AMPT and UrQMD models. It is observed that no models correctly describe the collision data. All the models, i.e. HIJING, AMPT and UrQMD, show a centrality independent behavior. It is observed that the N_{N-part} -normalized enhancement, obtained from AMPT model, is higher than the data obtained from HIJING and UrQMD models. This could be because of the partonic degrees of freedom in AMPT model.

In Figure 5, N_{N-part} -normalized enhancement of Ξ and $\bar{\Xi}$ -baryons at $\sqrt{s_{NN}} = 200$ GeV for Au+Au collisions is shown as a function of N_{N-part} . The left panel corresponds to Ξ and the right panel corresponds to $\bar{\Xi}$. The

collision data points, obtained from STAR experiment [20], are compared with HIJING, AMPT and UrQMD models. The enhancement observed from the model estimates are independent of centrality and are much less than the data (enhancement factor being close to one). Although AMPT model has partonic degrees of freedom, the enhancement of Ξ and $\bar{\Xi}$ being close to one, like HIJING and UrQMD models, indicate that AMPT model doesn't describe the enhancement of baryons of higher strangeness content and works like a hadronic model for multi-strange particles.

The collision data obtained from STAR experiment [20] on N_{N-part} -normalized enhancement of $\Omega + \bar{\Omega}$ -baryons at $\sqrt{s_{NN}} = 200$ GeV for Au+Au collisions are shown in Figure 6 as a function of N_{N-part} and are compared with the corresponding estimates of HIJING, AMPT and UrQMD models. The enhancement observed from HIJING and AMPT models are independent of centrality and the enhancement factor is close to one. Whereas the corresponding estimates from UrQMD show a rise with centrality like experimental data, only difference being the enhancement factor is higher in case of data compared to UrQMD.

The enhancement ratio of baryons and anti-baryons is usually affected by the net-baryon content or baryon stopping at mid-rapidity. This difference decreases with increase in collision energy. For this reason, the enhancement of baryons and anti-baryons are different at SPS energies which is not that much at RHIC energies. In Figure 7 and Figure 8, N_{N-part} -normalized enhancement of Λ and $\bar{\Lambda}$ -baryons for Pb+Pb collisions at $\sqrt{s_{NN}} = 17.3$ GeV are plotted as a function of N_{N-part} , respectively. The collision data at $\sqrt{s_{NN}} = 17.3$ GeV are from SPS WA97/NA57 experiments [21] and are compared with the corresponding estimates of HIJING, AMPT and UrQMD models, as shown in Figure 7 and Figure 8. The HIJING and AMPT data show a centrality independent behavior, whereas UrQMD shows a weak centrality dependence. But the collision data of Λ show a remarkable centrality dependence, as shown in Figure 7. At the same time the collision data, HIJING, AMPT and UrQMD data of $\bar{\Lambda}$ are almost independent of centrality, as shown in Figure 8. The difference in behavior of Λ and $\bar{\Lambda}$ at $\sqrt{s_{NN}} = 17.3$ GeV could be due to the different production mechanism. This difference in the production mechanism of $\bar{\Lambda}$ has been assigned to the following reasons. Firstly, the production threshold for anti-hyperons is larger than hyperons. Secondly, while going from higher to lower collision energy, baryon density of the system increases. This doesn't favor the production of particles without having a common valence quark with nucleons [21]. This difference in yields go away as one moves from SPS energy to top RHIC energy.

In Figure 9 and Figure 10, N_{N-part} -normalized enhancement of Ξ and $\bar{\Xi}$ -baryons at $\sqrt{s_{NN}} = 17.3$ GeV for Pb+Pb collisions for SPS data have been shown as a function of N_{N-part} . These data points are from WA97/NA57 experiments and are compared with the

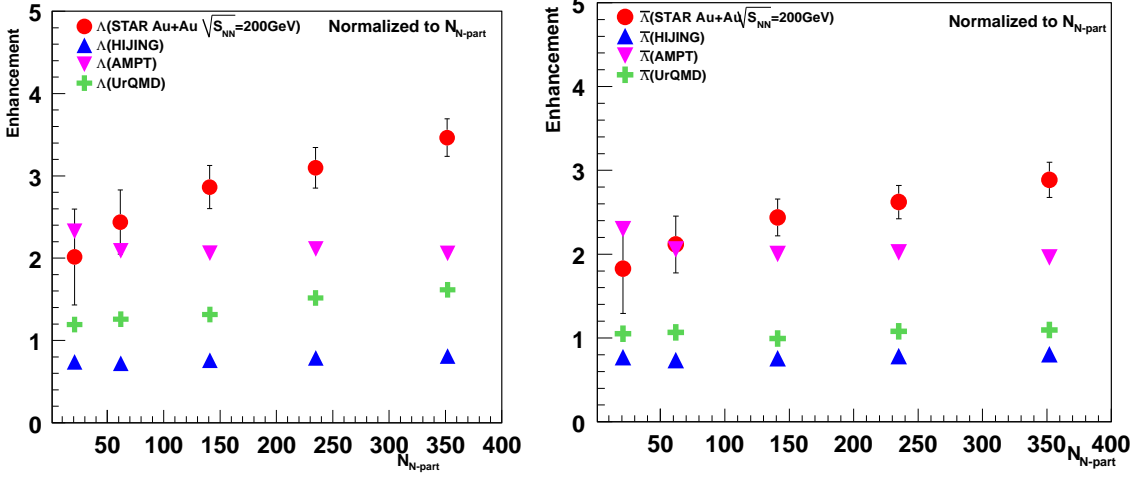


FIG. 4: (Color online) N_{N-part} -normalized enhancement of Λ (left) and $\bar{\Lambda}$ (right) as a function of collision centrality for Au+Au collisions at $\sqrt{s_{NN}} = 200$ GeV are compared with HIJING, AMPT and UrQMD models at mid-rapidity.

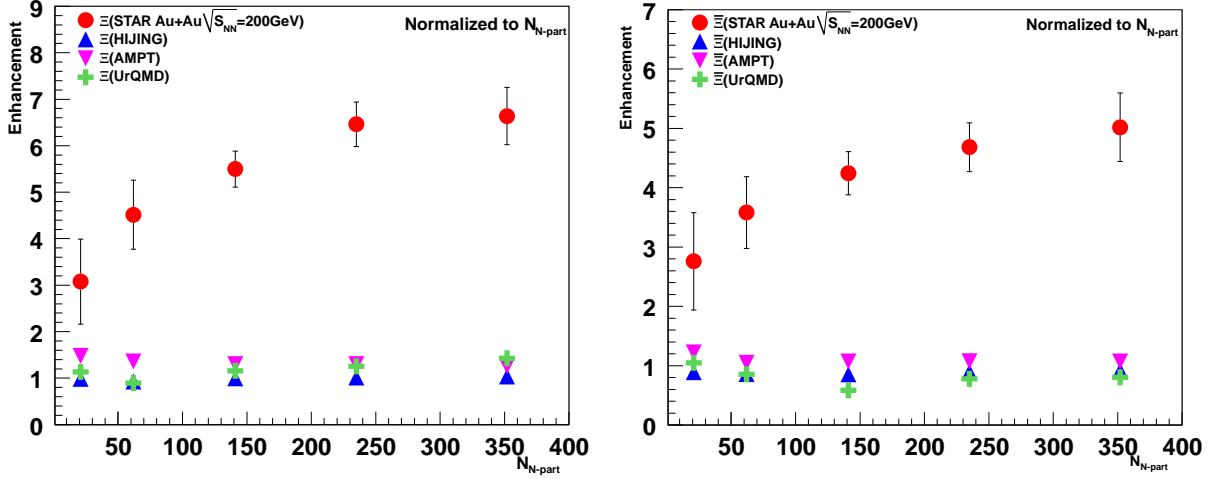


FIG. 5: (Color online) N_{N-part} -normalized enhancement of Ξ (left) and $\bar{\Xi}$ (right) as a function of collision centrality for Au+Au collisions at $\sqrt{s_{NN}} = 200$ GeV are compared with HIJING, AMPT and UrQMD models at mid-rapidity.

corresponding estimates of HIJING, AMPT and UrQMD models [21]. At SPS energies, both Ξ and $\bar{\Xi}$ show strangeness enhancement which rises with centrality, unlike the models under discussion. However, all the models with partonic and hadronic degrees of freedom show no enhancement of Ξ and $\bar{\Xi}$ -baryons and are independent of collision centrality.

In Figure 11, N_{N-part} -normalized enhancement of $\Omega + \bar{\Omega}$ -baryons at $\sqrt{s_{NN}} = 17.3$ GeV for Pb+Pb collisions have been shown as a function of N_{N-part} . These data points are from WA97/NA57 experiments and are compared with the corresponding estimates of HIJING, AMPT and UrQMD models [21]. A similar observation has been made for $\Omega + \bar{\Omega}$ -baryons like the Ξ -baryons.

To understand different enhancement profiles of multi-strange baryons at SPS energies, it is important to study their production dynamics. However, it could be observed that the shape of the enhancements for (anti) baryons are similar, which goes inline with the predictions of a grand canonical ensemble approach (GC) [28].

In Figure 12, N_{q-part} -normalized enhancement for multi-strange baryons for Au+Au collisions at $\sqrt{s_{NN}} = 200$ GeV have been shown as a function of collision centrality. These data points are from the STAR experiment at RHIC [20]. Here we observe that when the enhancement is normalized to the number of constituent quarks, it turns out to be a centrality independent scaling behavior. This enhancement, however, depends on the par-

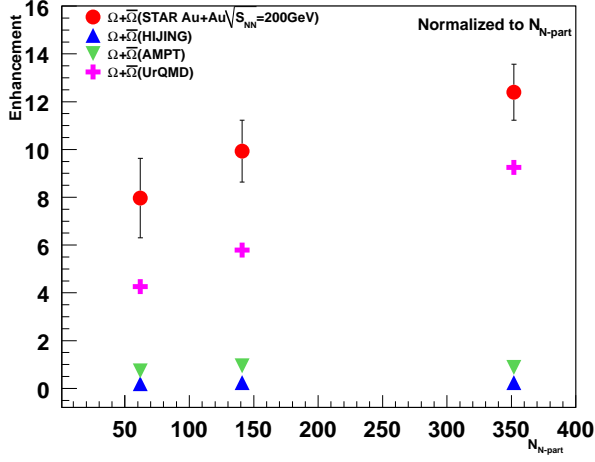


FIG. 6: (Color online) N_{N-part} -normalized enhancement of $\Omega + \bar{\Omega}$ as a function of collision centrality for Au+Au collisions at $\sqrt{s_{NN}} = 200$ GeV are compared with HIJING, AMPT and UrQMD models at mid-rapidity.

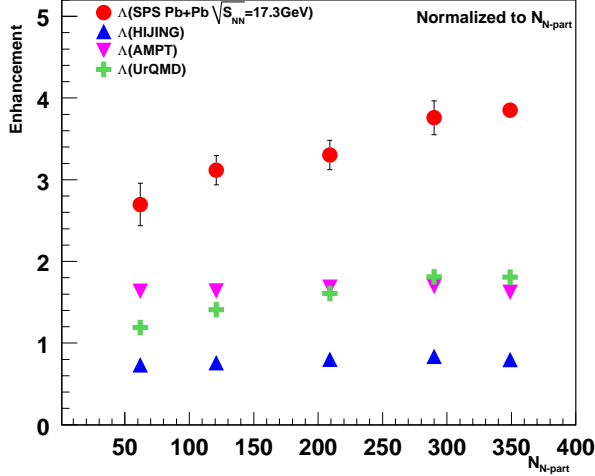


FIG. 7: (Color online) N_{N-part} -normalized enhancement of Λ as a function of collision centrality for Pb+Pb collisions at $\sqrt{s_{NN}} = 17.3$ GeV are compared with HIJING, AMPT and UrQMD models at mid-rapidity.

ticle mass with an increase with higher mass number. The former observation is very interesting in view of partonic degrees of freedom playing a crucial role in particle production especially for the multi-strange particles, the enhancement of which has been conjectured to be a signal of formation of a partonic phase. In other words, at top RHIC energy the collision could be described at a partonic level interactions. The number of quark participant scaling (NQ-scaling) works fine at intermediate p_T for the elliptic flow of multi-strange particles, showing partonic collectivity at RHIC [29]. This supports present observation of centrality independent scaling behavior of constituent quarks normalized multi-strange baryon en-

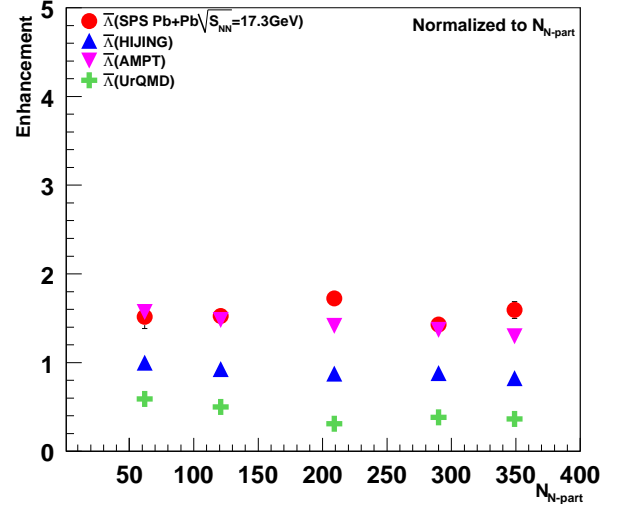


FIG. 8: (Color online) N_{N-part} -normalized enhancement of $\bar{\Lambda}$ as a function of collision centrality for Pb+Pb collisions at $\sqrt{s_{NN}} = 17.3$ GeV are compared with HIJING, AMPT and UrQMD models at mid-rapidity.

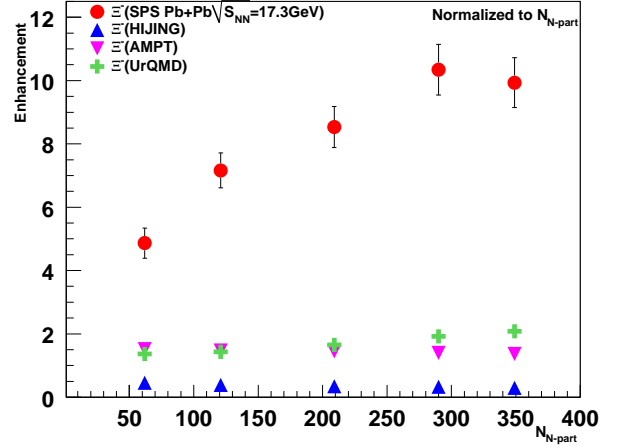


FIG. 9: (Color online) N_{N-part} -normalized enhancement of Ξ as a function of collision centrality for Pb+Pb collisions at $\sqrt{s_{NN}} = 17.3$ GeV are compared with HIJING, AMPT and UrQMD models at mid-rapidity.

hancement. This is also true at top SPS energy which is shown in Figure 13. Hence, it could be inferred here that a deconfinement phase transition might have taken place already at top SPS energies. This goes inline with other experimental findings on the onset of deconfinement or saturation of different observables starting from SPS energies [30, 31].

In Figure 13, N_{q-part} -normalized enhancement for multi-strange baryons at $\sqrt{s_{NN}} = 17.3$ GeV for Pb+Pb collisions have been shown as a function of collision centrality. These data points are from WA97/NA57 experiments [21]. Here, we observe that for lower strangeness content particles, the quark participant nor-

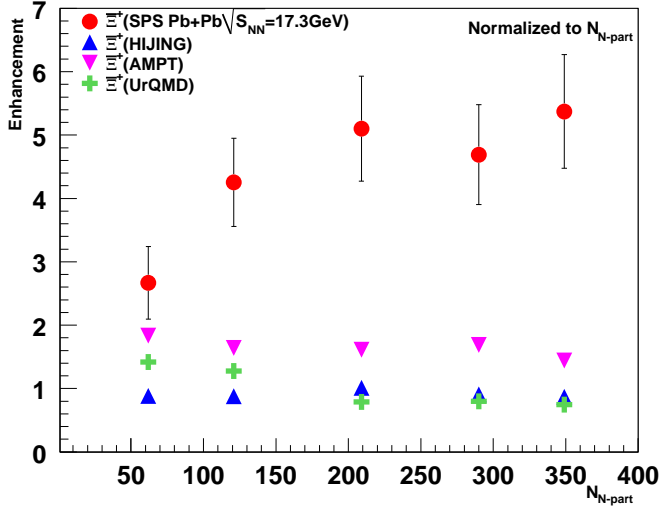


FIG. 10: (Color online) N_{N-part} -normalized enhancement of Ξ as a function of collision centrality for Pb+Pb collisions at $\sqrt{s_{NN}} = 17.3$ GeV are compared with HIJING, AMPT and UrQMD models at mid-rapidity.

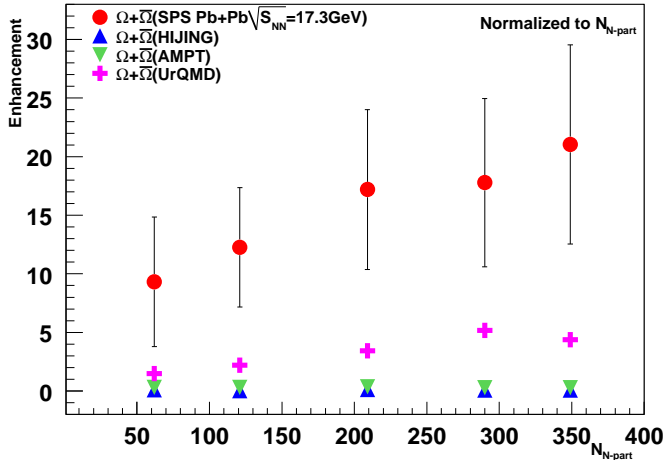


FIG. 11: (Color online) N_{N-part} -normalized enhancement of $\Omega + \bar{\Omega}$ as a function of centrality for Pb+Pb collisions at $\sqrt{s_{NN}} = 17.3$ GeV are compared with HIJING, AMPT and UrQMD models at mid-rapidity.

malized multi-strange enhancement turns out to be a centrality independent scaling-behavior. However, this is not true specifically for the Ω baryons, for which we observe a linear rise. This makes a difference between SPS and RHIC energies so far the constituent quark scaling of multi-strange baryons go.

The absolute values of the enhancement factor (after normalizing to the number of constituent quarks) as a function of strangeness content of different multi-strange baryons at top RHIC and SPS energies are shown in Figures 14 and 15, respectively. It is evident from these plots

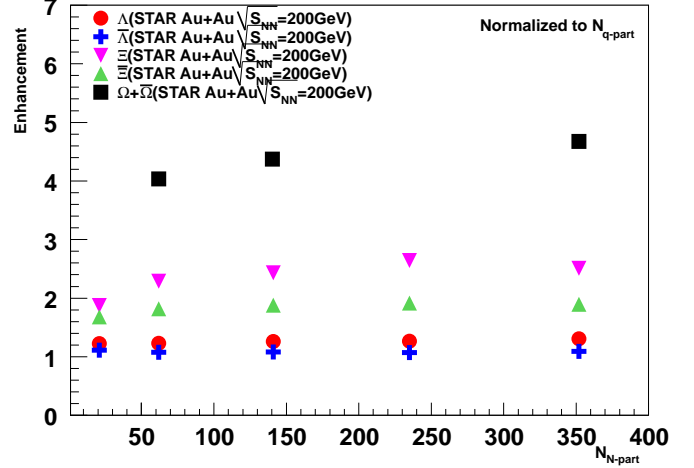


FIG. 12: (Color online) Mid-rapidity N_{q-part} -normalized enhancement of multi-strange baryons as a function of centrality for Au+Au collisions at $\sqrt{s_{NN}} = 200$ GeV at RHIC.

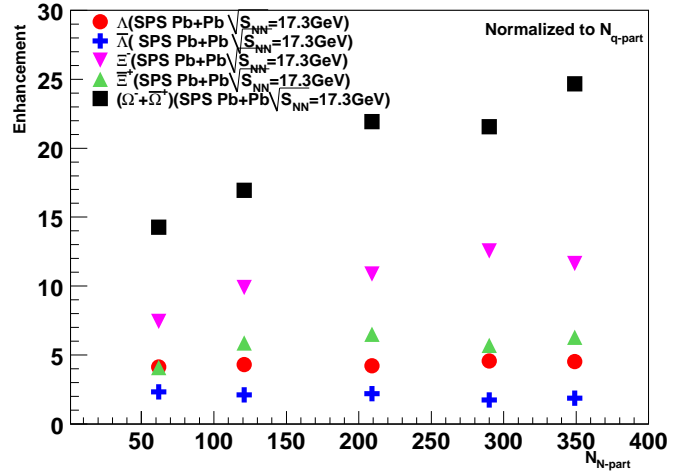


FIG. 13: (Color online) Mid-rapidity N_{q-part} -normalized enhancement of multi-strange baryons as a function of centrality for Pb+Pb collisions at $\sqrt{s_{NN}} = 17.3$ GeV at SPS.

that the absolute enhancement number decreases with collision energy. This could be understood in a grand canonical ensemble approach, which predicts a significant decrease in (anti) baryon enhancements with collision energy [20, 28]. We do observe a linear rise of the number of constituent quarks normalized strangeness enhancement as a function of strangeness content for both the energies. However, when we further normalize the enhancement factor with respect to the strangeness content and plot as a function of the strangeness content, we observe that it has a linear rise for top SPS energy, whereas it remains almost flat for the top RHIC energy. This means at top most RHIC energy both constituent quark and strangeness scaling of multi-strange baryons

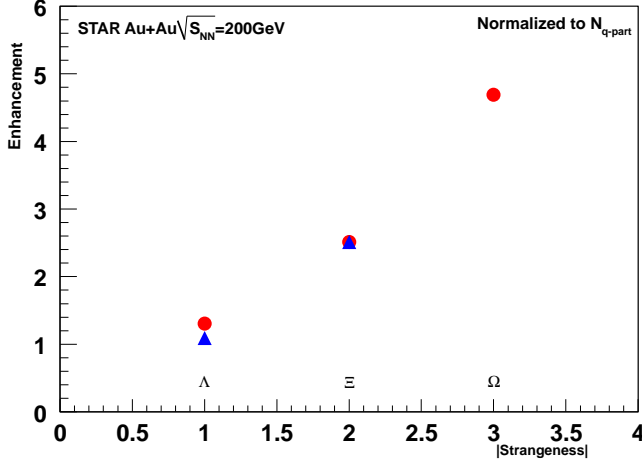


FIG. 14: (Color online) Mid-rapidity N_{q-part} -normalized enhancement of multi-strange baryons as a function of strangeness content for Au+Au collisions at $\sqrt{s_{NN}} = 200$ GeV at RHIC. The filled circles and triangles are for the particles and anti-particles, respectively.

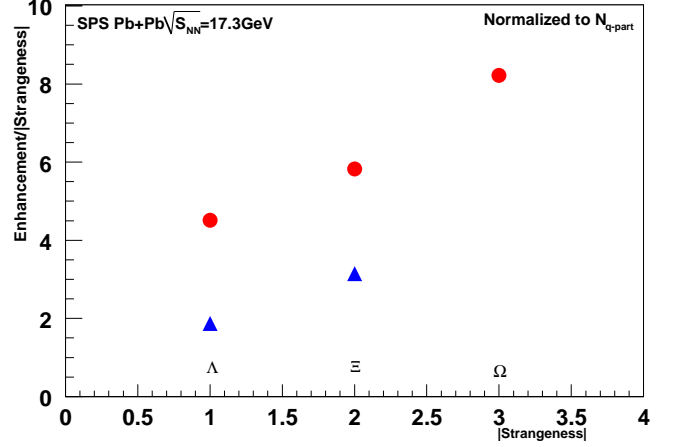


FIG. 16: (Color online) Mid-rapidity N_{q-part} and strangeness content normalized enhancement of multi-strange baryons as a function of strangeness content for Pb+Pb collisions at $\sqrt{s_{NN}} = 17.3$ GeV at SPS. The filled circles and triangles are for the particles and anti-particles, respectively.

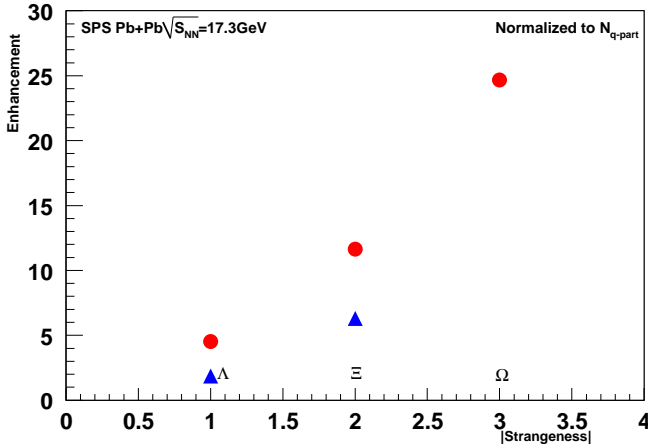


FIG. 15: (Color online) Mid-rapidity N_{q-part} -normalized enhancement of multi-strange baryons as a function of strangeness content for Pb+Pb collisions at $\sqrt{s_{NN}} = 17.3$ GeV at SPS. The filled circles and triangles are for the particles and anti-particles, respectively.

have been observed, which is of paramount importance in view of the formation of a partonic phase at RHIC. These are shown in Figures 16 and 17. We expect that these scaling laws will hold good at LHC energies.

IV. SUMMARY AND CONCLUSION

In this work, we have calculated the number of nucleon and quark participants in a proton-proton, proton-nucleus and nucleus-nucleus collisions, in the framework of a nuclear overlap model. The data for the enhance-

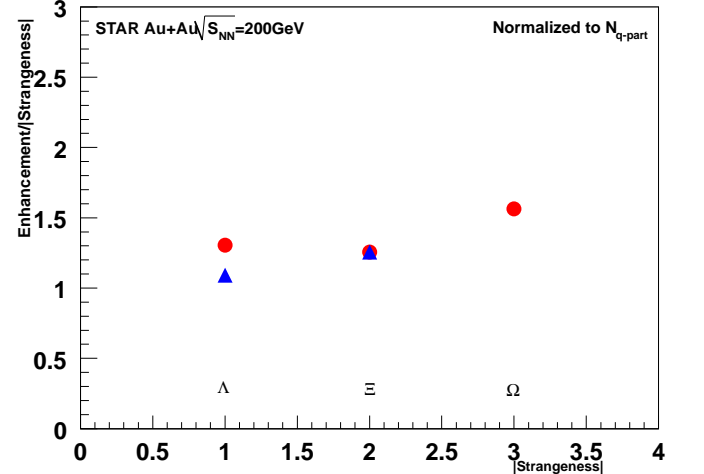


FIG. 17: (Color online) Mid-rapidity N_{q-part} and strangeness content normalized enhancement of multi-strange baryons as a function of strangeness content for Au+Au collisions at $\sqrt{s_{NN}} = 200$ GeV at RHIC. The filled circles and triangles are for the particles and anti-particles, respectively.

ment of multi-strange baryons at top SPS and RHIC energies have been compared with HIGING, UrQMD and AMPT models. We observe the N_{q-part} -normalized yields of multi-strange particles show a linear rise with centrality. This turns out to be a centrality independent scaling behavior when normalized to number of constituent quarks participating in the collision. This geometrical scaling indicates the partonic degrees of freedom playing important role in the production of multi-strange particles. Furthermore, we see the constituent quark normalized yield when further divided by the strangeness

content, it shows a strangeness independent scaling behavior at the top RHIC energy, whereas this scaling is not seen at the top SPS energy. This goes inline with other observations at RHIC towards the formation of a strongly coupled partonic phase called sQGP. These features are reproduced neither by explicit hadronic kinetic models like UrQMD, HLJING nor by AMPT model which treats the partonic phase on the basis of pQCD with massless

partons and a noninteracting equation-of-state.

Acknowledgments

Authors would like to thank Dr. Dariusz Miskowiec, GSI, Germany for fruitful discussions on the nuclear overlap model and Prof. R. Varma, IIT Bombay for useful discussions.

-
- [1] P. Koch, B. Muller and J. Raffelski, *Phys. Rep.* **142**, 167 (1986).
 - [2] L. McLerran, *Nucl. Phys. A* **461**, 245c (1987).
 - [3] H. van Hecke, H. Sorge and N. Xu, *Phys. Rev. Lett.* **81**, 5764 (1998).
 - [4] F. Karsch, *Prog. Part. Nucl. Phys.* **62**, 503 (2009); Z. Fodor and S. Katz, *J. High Energy Phys.* **04**, 050 (2004).
 - [5] Johann Rafelski and Berndt Muller, *Phys. Rev. Lett.* **48**, 1066 (1982).
 - [6] H. van Hecke, H. Sorge and N. Xu, *Phys. Rev. Lett.* **81**, 5764 (1998).
 - [7] S.F. Biagi *et al.*, *Nucl. Phys. B* **186**, 1 (1981).
 - [8] Y. Cheng *et al.*, *Phys. Rev. C* **68**, 034910 (2003).
 - [9] S.A. Bass *et al.*, *Phys. Rev. C* **60**, 021902 (1999); A. Dumitru *et al.*, *Phys. Lett. B* **460**, 411 (1999); S.A. Bass and A. Dumitru, *Phys. Rev. C* **61**, 064909 (2000).
 - [10] R.A. Muller, *Phys. Lett. B* **38**, 123 (1972).
 - [11] R.C. Hwa and C.S. Lam, *Phys. Rev. D* **26**, 2338 (1982).
 - [12] V.V. Anisovich, *Phys. Lett. B* **57**, 87 (1975); V.V. Anisovich *et al.*, *Nucl. Phys. B* **133**, 477 (1978).
 - [13] J. Adams *et al.* (STAR Collaboration), *Phys. Rev. Lett.* **95**, 122301 (2005).
 - [14] V.V. Anisovich, M.N. Kobylnsky, J. Nyiri and Y.M. Shabelsky, *Quark Model and High Energy Collisions* (World Scientific, Singapore, 1985).
 - [15] S. Eremín and S. Voloshin, *Phys. Rev. C* **67**, 064905 (2003).
 - [16] P. K. Netrakanti and B. Mohanty, *Phys. Rev. C* **70**, 027901 (2004).
 - [17] E. Shuryak, *Phys. Lett. B* **486**, 378 (2000).
 - [18] Rachid Nouicer, *AIP Conf. Proc.* **828**, 11 (2006) and Preprint nucl-ex/0512044.
 - [19] F. Becattini and G. Pettini, *Phys. Rev. C* **67**, 015205 (2003).
 - [20] B.I. Abelev *et al.* (STAR Collaboration), *Phys. Rev. C* **77**, 044908 (2008).
 - [21] E. Andersen *et al.* (WA97 Collaboration), *Phys. Lett. B* **449**, 401 (1999); F. Antinori *et al.* (WA97/NA57 Collaboration), *Nucl. Phys. A* **698**, 118c (2002).
 - [22] Bhaskar De and S. Bhattacharyya, *Phys. Rev. C* **71**, 024903 (2005).
 - [23] C.Y. Wong, *Introduction to High-Energy Heavy Ion Collisions* (World Scientific, 1994) p. 161.
 - [24] J. Adams *et al.* (STAR Collaboration), *Phys. Rev. C* **70**, 054907 (2004).
 - [25] Miklos Gyulassy and Xin-Nian Wang, *Comput. Phys. Commun.* **83**, 307 (1994).
 - [26] B. Zhang *et al.*, *Phys. Rev. C* **61**, 067901 (2000).
 - [27] S.A. Bass *et al.*, *Prog. Part. Nucl. Phys.* **41**, 225 (1998).
 - [28] J. Cleymans, K. Redlich and E. Suhonen, *Z. Phys. C* **51**, 137 (1991); K. Redlich and A. Tounsi, *Eur. Phys. J. C* **24**, 589 (2002).
 - [29] J. Adams *et al.* (STAR Collaboration), *Phys. Rev. Lett.* **95**, 122301 (2005).
 - [30] M. Gazdzicki, M. Gorenstein and P. Seyboth, *Acta Physica Pol. B* **42**, 307 (2011).
 - [31] J. Cleymans *et al.*, *Phys. Lett. B* **660**, 172 (2008).